

# HIGH FIDELITY COMPUTATIONAL FLUID DYNAMICS FOR MIXING IN WATER DISTRIBUTION SYSTEMS

**Stephen W. Webb and Bart G. van Bloemen Waanders**

Sandia National Laboratories

Albuquerque, New Mexico

[swwebb@sandia.gov](mailto:swwebb@sandia.gov)

## Abstract

*Network simulation models for water distribution systems typically assume the mixing at pipe intersections is complete and instantaneous. More accurate characterizations of chemical or biological agent transport may be required to efficiently identify, control and mitigate the spread of harmful agents and to protect critical components within the network. Recent experimental data have shown that mixing is incomplete at pipe junctions (pipe crosses and tees). Numerical simulations of these experiments have been performed using simplified turbulence methods. In the present study, simulations of mixing in pipe junctions are performed using the high-fidelity Large Eddy Simulation (LES) approach to fully resolve the mixing behavior. Simulation results show unsteady mixing behavior at the fluid interface due to shear layer instabilities. These high-fidelity results will be used to develop a lower fidelity model for mixing at pipe junctions.*

## Keywords

network simulation models, EPANET, mixing, turbulence, computational fluid dynamics, pipe junctions

## 1. Introduction

Network simulation models are used to predict hydraulic behavior and chemical transport within water distribution systems in order to manage chlorine distribution, maintain water quality, and design network expansions. Tools such as EPANET (Rossman, 2000) have successfully been applied to a large range of datasets and validated with tracer and other field tests. The computational requirement associated with the size of these datasets necessitates the need to make simplifying assumptions about fluid flow. Standard network models typically assume the mixing at pipe intersections is complete and instantaneous. In the case of a cross-junction in which one inlet provides clean water and the other contaminated water, the outlets will be equally contaminated.

More accurate characterizations of chemical or biological agent transport may be required to efficiently identify, control and mitigate the spread of harmful agents and to protect critical components within the network. In the past, very little work has been performed to evaluate this mixing behavior. Fowler and Jones (1991) questioned the validity of the instantaneous mixing assumption for certain junctions in water distribution networks; however, no numerical studies were performed. More recently, numerical results showed the potential for incomplete mixing at pipe junctions and the need to accurately understand the flow characteristics (van Bloemen Waanders et al., 2005). Although the numerical results compared favorably to preliminary experimental data, the numerical results were considered qualitative because of a few shortcomings with the numerical model. More recently, Ho et al. (2006) and Choi et al. (2006) have performed experiments and numerical simulations of mixing at pipe junctions. Both of these studies used a steady Reynolds-Averaged Navier Stokes (RANS) turbulence model to predict the

mixing in the pipe junctions. The incomplete mixing data are fit to the experimental data by varying the turbulent Schmidt number.

In the present study, simulations of mixing in pipe junctions (pipe cross and tees) are performed using the high-fidelity Large Eddy Simulation (LES) approach to fully resolve the mixing behavior. Turbulence in high Reynolds flow is the dominant flow characteristic that contributes to the overall mixing process (Blasek, 2001; Tennekes and Lumley, 1972). By resolving the temporal and spatial behavior of the mixing processes by using LES, we hope to extract certain fundamental mechanisms responsible for the mixing behavior including any unsteady characteristics. Once the fundamental mechanisms are understood, a lower fidelity model can be developed based on this understanding.

## **2. Model Development**

In order to simulate the mixing in a cross and tees, a high-fidelity three-dimensional model has been developed using FLUENT, a commercial computational fluid dynamics (CFD) code (Fluent, Inc., 2005a). The code simulates flow and heat transfer in fluids by solving the Navier-Stokes and energy conservation equations including turbulence. The selection of the turbulence approach is critical to fully resolving the fundamentals of the mixing behavior.

### **2.1 Turbulence**

There are numerous approaches to simulating turbulence (Pope, 2000). Traditional approaches such as steady Reynolds-Averaged Navier-Stokes (RANS) and unsteady RANS (URANS) solve for the time-averaged velocity by using two-equation ( $k$ - $\epsilon$  or  $k$ - $\omega$ ) turbulence approaches. These approaches are computationally efficient but are limited in their ability to fully resolve all the appropriate details associated with turbulence. More recently, the Large Eddy Simulation (LES) approach has been gaining popularity. In this case, the Navier Stokes equations are spatially filtered so the fluid velocity is explicitly resolved down to the scale of the grid. In this way, large eddies are directly simulated. Small eddies, or eddies smaller than the mesh size, are modeled through a subgrid scale turbulence model. LES requires much more computational resources than steady RANS or URANS approaches due to the finer mesh required, but the results are much more realistic for complex situations and will be used for the present high-fidelity simulations.

All three approaches (RANS, URANS, LES) to calculating turbulence start with the instantaneous Navier-Stokes equations. However, the resulting turbulence equations are fundamentally different. In RANS and URANS, the instantaneous velocity is decomposed into a time-averaged velocity and a fluctuating velocity. Turbulence is modeled as a function of the fluctuating velocities, and the evolution of the time-averaged velocity is simulated. In steady RANS, the time-averaged velocity is simulated (resolved) and the velocity fluctuations are modeled (unresolved) through turbulence models. In URANS, the time-averaged velocity and some of the lower frequency unsteady behavior are simulated; the high frequency turbulent velocity fluctuations are modeled. In LES, the velocity is also decomposed. However, in this case, the decomposition is made through a spatial filter such that the velocity decomposition is the resolved velocity, or that which can be simulated down to the grid scale, and the residual, or unresolved velocity, which is modeled at the subgrid scale. The motion of the large eddies, relative to the grid, are simulated by the conservation equations. The rationale for LES is that momentum, mass, and passive scalars are mostly transported by large eddies, which are more problem dependent and are dictated by the geometry of the flow and boundary conditions. The

smaller eddies are less dependent on problem specific conditions and are more isotropic, so they can be modeled through a defined relationship, or subgrid scale turbulence model, with more confidence. The entire frequency spectrum of the velocity fluctuations due to external events and turbulence is directly simulated up to the frequency cutoff due to the size of the grid. As the grid is refined, the resolved frequency range becomes larger and the unresolved subgrid scale turbulence becomes smaller and smaller, eventually going to zero as all frequencies are simulated and Direct Numerical Simulation (DNS) is approached.

As mentioned above, all three approaches decompose the actual fluid velocity. In LES, the velocity is decomposed into a filtered (resolved) velocity and a fluctuating (unresolved) component as follows

$$u_i = \bar{u}_i + u_i'$$

The fundamental conservation equations for continuity and momentum are given below

Continuity

$$\frac{\partial \rho}{\partial t} + \frac{\partial}{\partial x_i} (\rho \bar{u}_i) = 0$$

Momentum

$$\frac{\partial}{\partial t} (\rho \bar{u}_i) + \frac{\partial}{\partial x_j} (\rho \bar{u}_i \bar{u}_j) = \frac{\partial}{\partial x_i} \left( \mu \left( \frac{\partial \sigma_{ij}}{\partial x_j} \right) \right) - \frac{\partial \bar{p}}{\partial x_i} - \frac{\partial \tau_{ij}}{\partial x_j}$$

Stress tensor due to molecular viscosity

$$\sigma_{ij} = \left[ \mu \left( \frac{\partial \bar{u}_i}{\partial x_j} + \frac{\partial \bar{u}_j}{\partial x_i} \right) \right] - \frac{2}{3} \mu \frac{\partial \bar{u}_l}{\partial x_l} \delta_{ij}$$

Turbulent stress

$$\tau_{ij} = \overline{\rho u_i u_j} - \rho \bar{u}_i \bar{u}_j$$

These equations are exactly the same as for RANS approaches except for the turbulent stress equation and the definition of the velocity. Rather than a time-averaged value that is used in RANS, LES resolves the fluid velocity down to the grid scale.

For LES, the subgrid scale model is

$$\tau_{ij} - \frac{1}{3} \tau_{kk} \delta_{ij} = -2 \mu_t \bar{S}_{ij}$$

$$\overline{S}_{ij} = \frac{1}{2} \left( \frac{\partial \overline{u}_i}{\partial x_j} + \frac{\partial \overline{u}_j}{\partial x_i} \right)$$

The Smagorinski model (Smagorinski, 1963) is the most widely-used LES subgrid scale model

$$\mu_t = \rho L_s^2 |\overline{S}|$$

$$|\overline{S}| = \sqrt{2 \overline{S}_{ij} \overline{S}_{ij}}$$

$L_s$  is a length scale. Fluent calculates the value as follows

$$L_s = \min(\kappa d, C_s V^{1/3})$$

where  $\kappa$  is the von Karman constant,  $d$  is the distance to the closest wall,  $C_s$  is the Smagorinski constant, and  $V$  is the computational cell volume. The present simulations use the dynamic Smagorinski model, where the constant  $C_s$  is based on local conditions as detailed in Kim (2004).

The equations for species transport without reactions or sources terms are:

$$\frac{\partial}{\partial t}(\rho Y) + \frac{\partial}{\partial x_i}(\rho \overline{u}_i Y) = -\frac{\partial J_i}{\partial x_i}$$

$$J_i = -\left( \rho D + \frac{\mu_t}{Sc_t} \right) \frac{\partial Y}{\partial x_i}$$

The influence of the turbulent Schmidt number,  $Sc_t$ , is significantly different for RANS models (including URANS) and for LES. In RANS, most of the turbulence is modeled rather than simulated, so the ratio of  $\mu_t / Sc_t$  will be large and will often overwhelm the laminar contribution. In LES, the ratio of  $\mu_t / Sc_t$  will be much smaller than in RANS and will be a function of the grid size as can be seen from the Smagorinski subgrid scale model equations above through the length scale. In fact, as the grid gets smaller and smaller and goes toward Direct Numerical Simulation (DNS), the turbulent viscosity goes to zero, all the mixing is explicitly resolved by the simulations, and there is no effect of the turbulent Schmidt number. Therefore, values of the turbulent Schmidt number are not transferable between RANS and LES approaches.

The FLUENT CFD code has been validated for LES for a number of situations. Successful data-model comparisons have been conducted for fully-developed channel flow, flow over a square cylinder, flow over a sphere, flow and heat transfer over isolated circular cylinders, and flow in tube bundles (Kim, 2004, Kim and Mohan, 2005, Kim, 2006, Kim and Nakamura, 2006, Webb and Cook, 2006).

## 2.2 Simulation Model

In the laboratory experiments (Ho et al., 2006), a cross or double-sided tee are used with long upstream and downstream pipe runs. One inlet branch has a salt tracer, and the tracer distribution in the two outlet branches is measured to evaluate the mixing in the cross or tee. The long inlet pipe runs result in fully-developed inlet flow conditions. Rather than simulating the long upstream pipe runs or specifying an arbitrary inlet boundary condition, a small periodic model of pipe flow is used to calculate fully-developed LES conditions for the inlets. The geometric setup of the CFD model is shown in Figure 1 including the periodic inlet pipe sections.

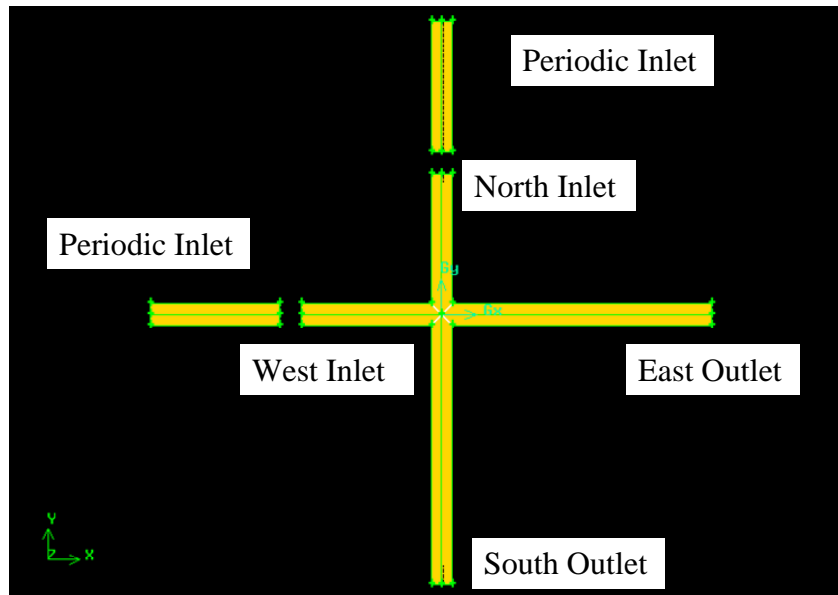


Figure 1  
Fluent Model Setup for Crosses

The periodic inlets are run independently of the full model. This setup is much more efficient than including them in the full model because fully-developed LES conditions, which can take some time to develop, are calculated without the need to simulate the entire cross model. Once these fully-developed LES conditions are established, they are fed directly into the cross model, thereby providing appropriate turbulence characteristics to the critical intersecting fluid interfaces.

A User Defined Function (UDF) was written for Fluent to take the results from the periodic inlet model after fully-developed conditions were established and write them to a file at every time step for every grid point on the inlet periodic mesh. These files are then used as input boundary conditions for the full model. Separate models/files were used for the two inlets to the cross to permit independent inlet variations. The meshes and the time steps in the periodic inlet models and the cross inlets are required to be the identical.

For the present simulations, the pipe diameter is 2 inches, and the Reynolds number is 40,000 with nominal inlet mass flow rates of 1.6 kg/s. The fluid density and fluid viscosity have been assumed to be 998.2 kg/m<sup>3</sup> and 0.001003 Pa-s, respectively. The molecular diffusivity for the tracer-water mixture is 10<sup>-9</sup> m<sup>2</sup>/s. The default value of the turbulent Schmidt number of 0.7 has been used. Some simulations were also performed with the actual experimental mass flow rates,

which are somewhat different than the nominal values. The general behavior of the flow field, such as the velocity profile, velocity fluctuations, and shear stress, in these periodic inlet models compare favorably to literature data for pipe flow as given in AGARD (1998) and associated test cases for pipes and channels. Separate validation simulations for test case PCH03 for a Reynolds number of about 24,600 have been performed and show very good results.

Central differencing was used for momentum discretization, second order upwind was specified for energy discretization, and SIMPLEC was used for pressure-velocity coupling. A second-order temporal discretization scheme was used for all simulations. For the outlet boundary conditions, equal flow fractions for each outlet pipe were specified resulting in equal mass flow rate through both branches for the nominal flow case. For the actual flow case, the flow fractions from the data were used.

Two separate meshes were developed for the simulations. A coarse mesh was developed for preliminary simulations, while a fine mesh was made to resolve many of the details of the flow and to check for mesh convergence. The coarse mesh is shown in Figures 2 and 3. Figure 2 shows the cross/pipe intersection details on the mid-plane. The pipe cross model is broken up into 4 volumes based on the middle of the cross, so the mesh is symmetrical in all directions. The pipe and cross faces were paved and extruded to the inlets/outlets to complete the volume mesh. Figure 3 shows the mesh on the inlet face, which consists of a boundary layer mesh on the pipe walls and a paved mesh in the middle. The total number of cells in the cross section of the model is 128,900. Figures 4 and 5 show the details of the finer mesh with a total of 1,742,400 cells.

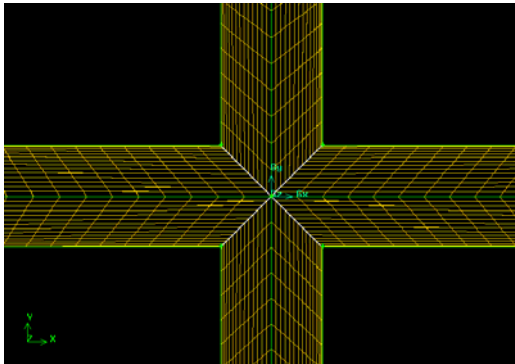


Figure 2  
Fluent Coarse Mid-Plane Mesh

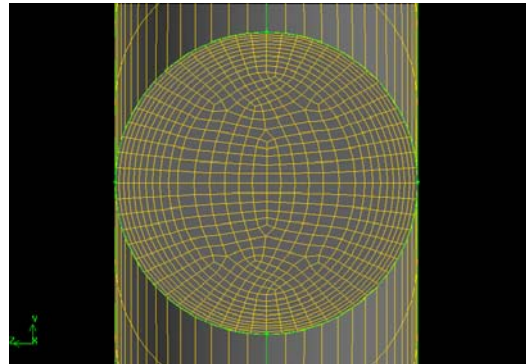


Figure 3  
Fluent Coarse Inlet Face Mesh

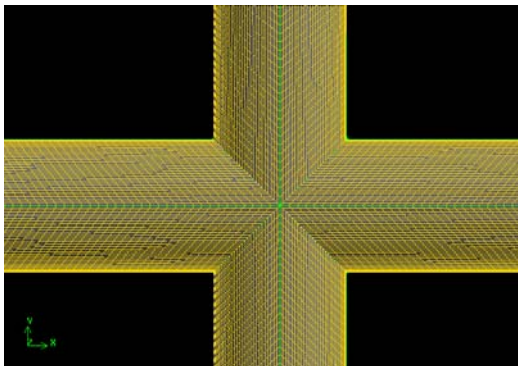


Figure 4  
Fluent Fine Mid-Plane Mesh

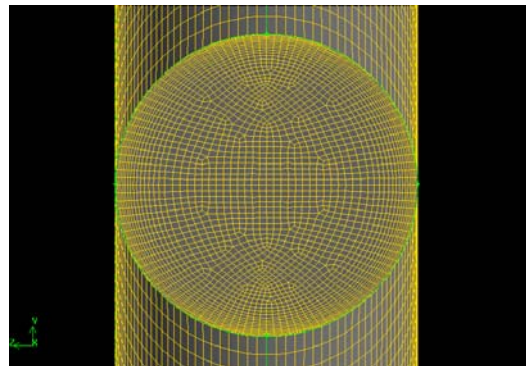


Figure 5  
Fluent Fine Inlet Face Mesh

One measure of mesh quality for turbulent flow is the  $y^+$  value, or the dimensionless distance of the first mesh point away from the wall

$$y^+ = \frac{y \sqrt{\tau_w / \rho}}{\nu}$$

where  $y$  is the physical distance of the first mesh point from the wall,  $\tau_w$  is the wall shear stress,  $\rho$  is the fluid density, and  $\nu$  is the fluid viscosity. For LES simulations, the  $y^+$  values should be about 1.0 (Fluent, 2005b). For the present meshes, the  $y^+$  values range between 4 and 10 for the coarse model, and between 2 and 6 for the fine model. The meshes will be further refined in subsequent simulations to approach the desired  $y^+$  values.

In addition to the crosses, preliminary simulations for double-sided tees at different separation distances have been performed using the coarse mesh. The two tees are on opposite sides. The primary reason for conducting laboratory and numerical experiments on tees was to evaluate the effects of retention time on mixing. The model for a separation distance (centerline to centerline) of 2.5 diameters is shown in Figure 6.

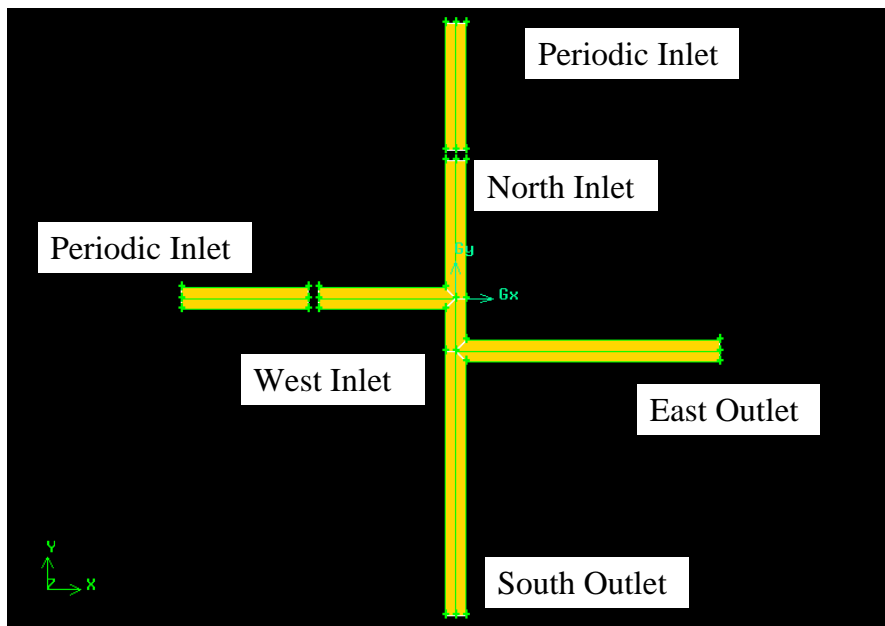


Figure 6  
Fluent Model Setup for Tees With 2.5D Separation

### 3. Results

#### 3.1 Cross

##### a. Fine Mesh

The fine mesh results will be discussed first because they demonstrate the detailed flow and mixing characteristic of the flow. The coarse results will be cited to confirm mesh convergence for the predicted mixing behavior.

Mixing in a cross is incomplete. Clean fluid enters the north inlet, while contaminated fluid enters the west inlet. The two streams seem to “bounce” off each other with a limited amount of mixing. The north inlet stream is generally deflected to the east outlet, while the west inlet stream is deflected to the south outlet. This behavior is qualitatively similar to that seen by Ashgriz et al. (2001) for two impinging jets at low flow rates. While the details of the flow and behavior after impingement are quite different, the fact that the two fluid streams seem to bounce off each other with limited mixing is similar.

The mass-averaged concentrations in the east and south outlets for the nominal flow rates are shown in Figure 7 as a function of time. For complete mixing, the mass fractions for both outlets would be 50%, or 0.5. The results show that about 91% of the contaminated water from the west inlet goes out the south outlet, while only about 9% goes out the east outlet. The oscillatory behavior of the outlet concentrations is due to unsteady mixing in the cross that is captured by the LES turbulence approach.

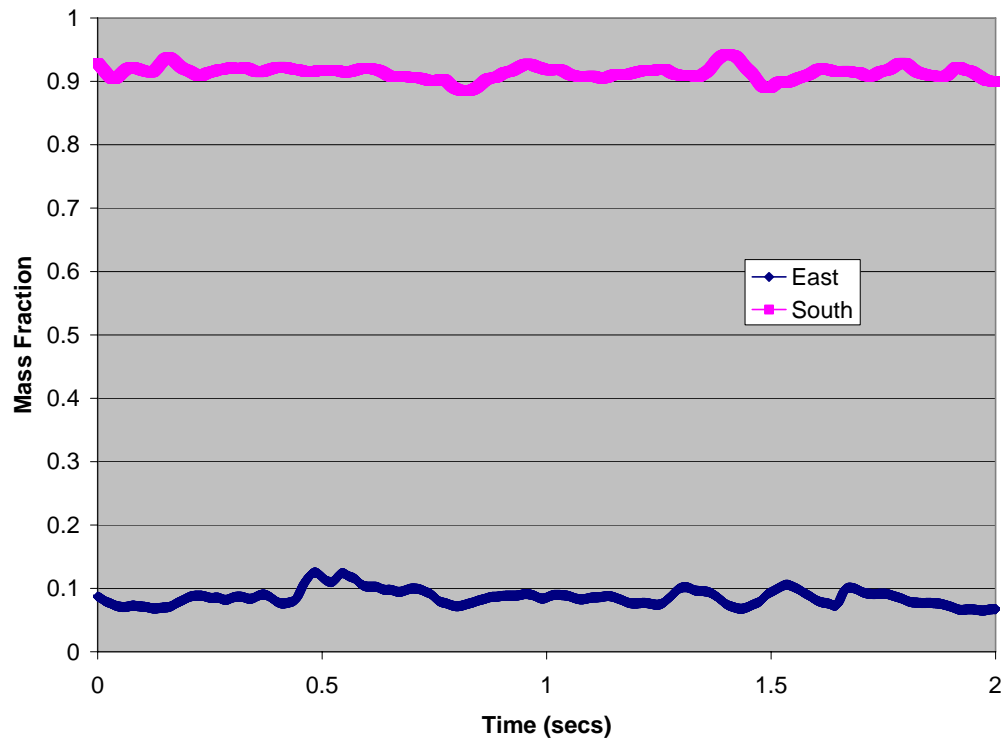
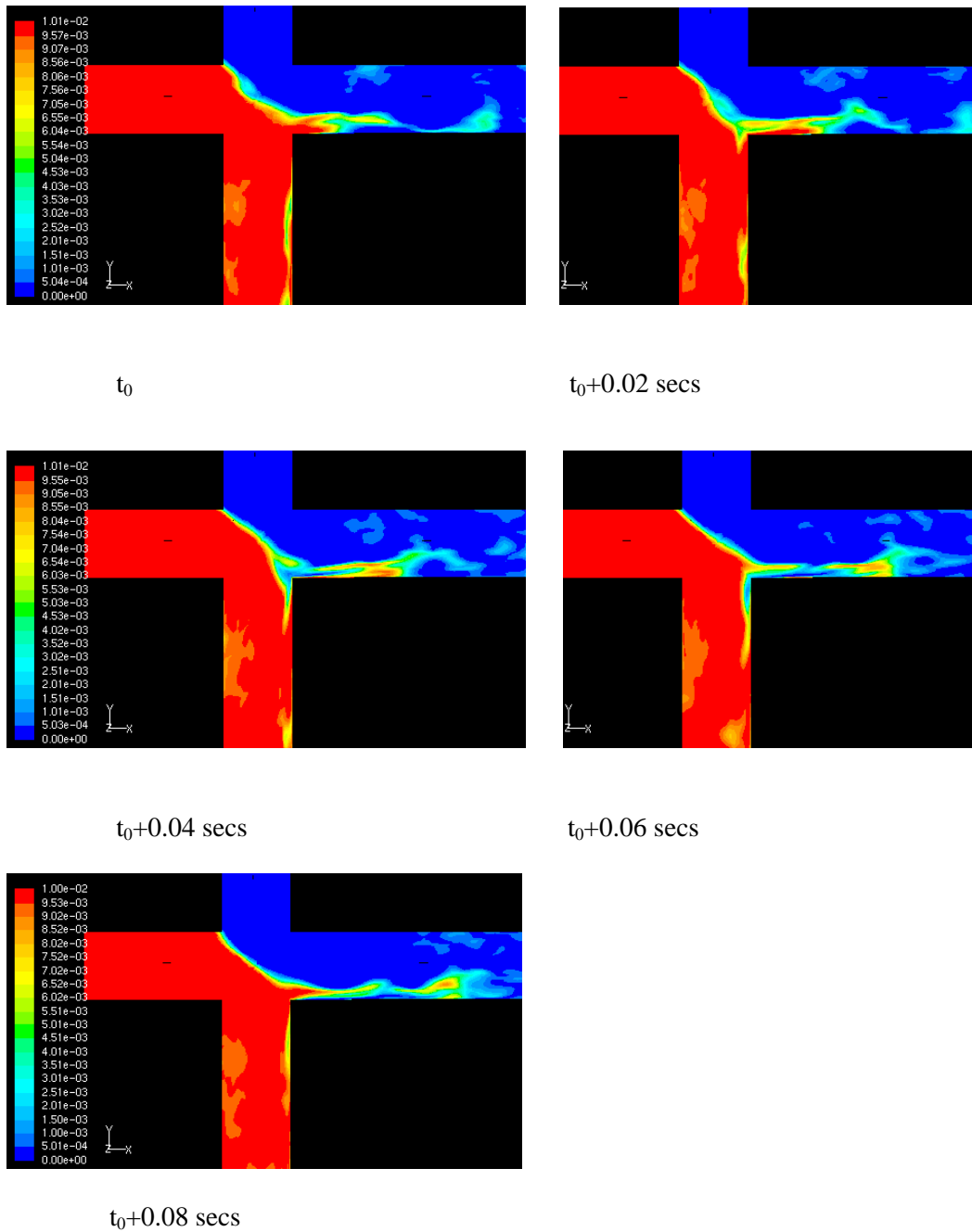


Figure 7  
Time-Dependent Outlet Normalized Concentrations for Nominal Flow Rates



**Figure 8**  
Unsteady Behavior of Mixing Interface

The behavior of the mixing interface between the clean and contaminated fluid is highly transient and is shown in Figure 8, where discrete snapshots of concentration contours on the center plane are shown. Each picture represents a time slice 0.02 seconds greater than the previous one. In the first picture, some of the contaminated fluid entering the west inlet goes into the east outlet leg. In the next two snapshots, the unsteady interface cuts off this fluid parcel, and essentially all of the contaminated fluid goes into the south leg. The following two pictures re-establish some contaminated fluid passing through to the east leg. The behavior of the interface then recycles back to the beginning of the sequence. The fluid crossing over (north to south; west to east) is not

continuous but is divided into discrete parcels due to the unsteady behavior of the interface. The behavior is similar to the interface between two shear layers. The interface oscillates at about 10 to 12 Hz based on these results.

The mixing split of 0.91-0.09 is slightly higher than the preliminary data that gave a 0.87-0.13 mixing split. The preliminary data were scoping experiments using the experimental setup described in Ho et al. (2006). One possibility is that the actual flow rates, which are different than the nominal values, may cause some of the difference. As mentioned earlier, the nominal (desired) flow rate is 1.6 kg/s through each inlet/outlet. The actual inlet flow rates in the north and west legs of the experiment were 1.57 and 1.594 kg/s, respectively. Because of experimental uncertainties, the outlet mass flow rate was a few percent larger than the inlet flow rate. The east flow rate was 1.507 kg/s, while the east value was 1.646 kg/s. The flow split between the east and south outlet legs was unequal due to differences in flow resistance caused by downstream fittings. Therefore, the inlet flow rates were honored, and the outlet flow rate fractions were specified so mass in and mass out are equal.

The effect of using the actual flow rates on the mixing behavior is minimal. Rather than a 0.91-0.09 split based on the nominal flow rates, the split was 0.90-0.10 using the actual flow rates. As discussed earlier, the experimental split was 0.87-0.13. Note that these data are preliminary and are being redone with better experimental controls of the experimental conditions and data.

#### **b. Coarse Mesh**

The results from the coarse mesh simulations agree very well with the fine mesh results indicating mesh convergence. The coarse mesh split for the nominal flow rates is 0.91-0.09, while the actual flow rate values are 0.90-0.10, or the same as the fine mesh to two decimal places. Therefore, the coarse mesh simulations can be used to estimate the mixing ratios in crosses and tees.

### **3.2 Tees**

Preliminary results using the coarse mesh have been conducted for two tee configurations with different separations as described earlier.

For the 2.5 diameter separation distance, a snapshot of the concentration contours is shown in Figure 9. The contaminated water coming in the west leg seems to hug the west side of the connecting leg, indicating that the orientation of the two tees may be important. The calculated flow split from these simulations is 0.59-0.41. The preliminary experimental data show a flow split of 0.68-0.26, which obviously is in error because the values do not add up to 1.0. These experiments are being redone.

Concentration contours are shown in Figure 10 for the 10 diameter separation distance model. While the contaminated water still tends to hug the west side of the connecting pipe, there is more mixing between the tees. The calculated flow split is 0.55-0.45 for this model. Experimental data are not available yet for this configuration.

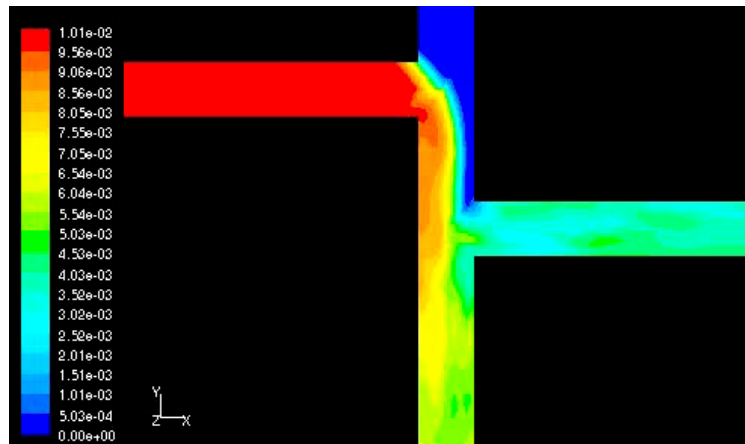


Figure 9  
Concentration Contours for 2.5D Separation Tee

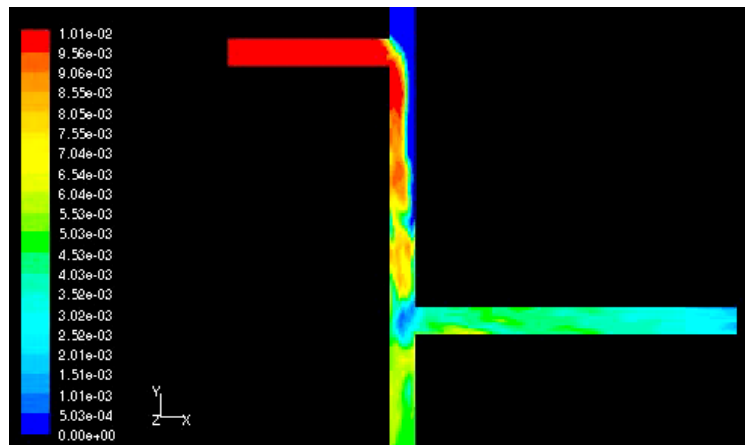


Figure 10  
Concentration Contours for 10D Separation Tee

#### 4. Summary and Discussion

High-fidelity LES simulations have been performed for 2 inch pipe intersections at a Reynolds number of 40,000. Cross and tee configurations with different separation distances have been simulated. The mixing is incomplete for the cross configuration with a split of 0.91- 0.09 for nominal flow rate conditions with the fine mesh (complete mixing would be 0.50-0.50), while the flow split is 0.90-0.10 for actual experimental flow rates (O'Rear et al., 2005). Coarse mesh values are the same to two decimal places. The preliminary experimental data indicate a flow split of 0.87-0.13. For tees, the mixing is much better. For tee separation distances of 2.5 and 10 diameters, the calculated mixing ratios are 0.59-0.41 and 0.55-0.45. These data are being redone as discussed by Ho et al. (2006). The data-model comparison is summarized in Figure 11. Mixing in the tees may be dependent on the orientation of the two tee sections because the flow seems to hug the inlet side of the tee similar to a wall jet. The attachment of the incoming stream at a tee configuration was also noted by Plesniak and Cusano (2005) as one of their flow regimes for mixing at a duct intersection.

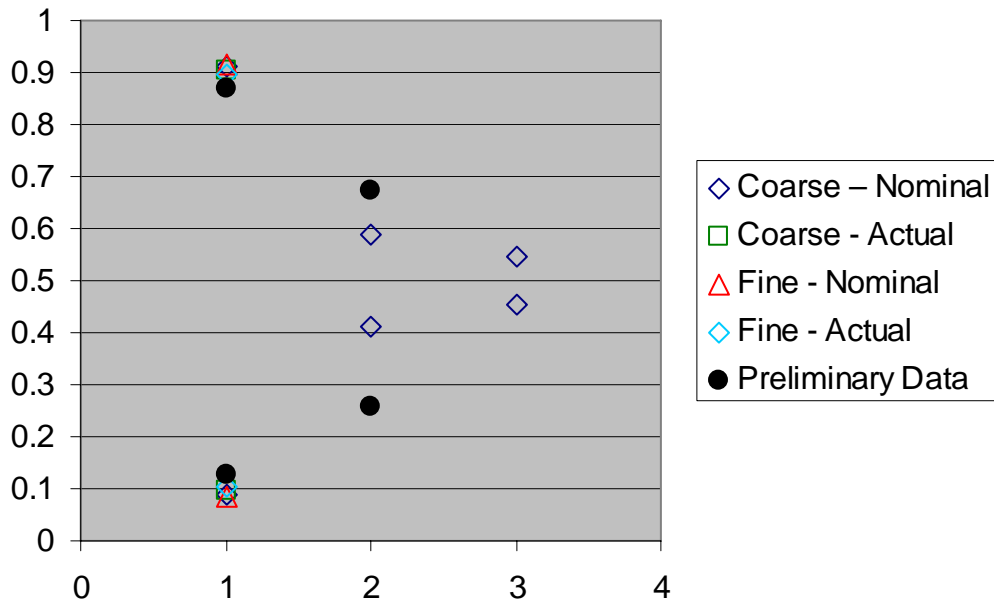


Figure 11  
Data-Model Comparison

Mixing at the interfaces in the crosses and tees is due to unstable interfacial behavior similar to shear layer instability. Using the high-fidelity LES turbulence model, the interface is highly transient with a frequency of about 10 to 12 Hz. Simplified models using RANS turbulence models (Ho et al., 2006; Choi et al, 2006) simulate a steady interface that is significantly different than the LES simulations.

The mixing across the shear layer interface is highly unsteady. Part of the unsteadiness is due to the turbulent velocity fluctuations in the inlet flow, which is naturally modeled using LES. For example, van Toonder et al. axial rms velocity fluctuations are approximately constant with Reynolds number and vary from about 38% of the local velocity near the wall to about 4% at the centerline (AGARD, 1998). These turbulent fluctuations are probably a significant contributor to the transient behavior of the mixing interface.

The correlation of mixing across the interface with the turbulent Schmidt number, as done by Ho et al, (2006) and Choi et al., (2006), is not directly comparable with the current LES model. As discussed earlier, the turbulent Schmidt number does not translate between RANS and LES approaches. A more fundamental correlation approach will be investigated in the future.

## Nomenclature

$C_s$	Smagorinski constant
$d$	distance to the closet wall
$D$	diffusivity
$L_s$	length scale
$p$	pressure
$S$	Mean rate-of-strain tensor
$Sc_t$	turbulent Schmidt number
$t$	time
$u$	fluid velocity
$\bar{u}$	filtered (resolved) fluid velocity
$u'$	fluctuating (unresolved) fluid velocity
$V$	computational cell volume
$y$	distance of the first mesh point to the wall
$Y$	tracer mass fraction

## Greek

$\rho$	fluid density
$\mu$	fluid dynamic viscosity
$\nu$	fluid kinematic viscosity ( $= \mu / \rho$ )
$\sigma$	stress tensor
$\tau$	shear stress
$\delta$	delta function
$\kappa$	von Karmen constant

## Subscripts

$i, j$	direction indice
$l$	direction indice
$t$	turbulent
$w$	wall

## Misc

$\bar{\quad}$	filtered value
---------------	----------------

## Acknowledgment

Sandia is a multiprogram laboratory operated by Sandia Corporation, a Lockheed Martin Company for the United States Department of Energy's National Nuclear Security Administration under contract DE-AC04-94AL85000.

## References

- AGARD, 1998, "A Selection of Test Cases for the Validation of Large-Eddy Simulations of Turbulent Flows," Advisory Group for Aerospace Research & Development, AGARD Advisory Report 345 (AGARD-AR-345), NATO.
- Ashgriz, N., W. Brocklehurst, and D. Talley, 2001, "Mixing Mechanisms in a Pair of Impinging Jets," *J. Propulsion and Power*, 17:736-749.
- Blazek, J., 2001, Computational Fluid Dynamics: Principles and Applications, Elsevier Science.
- Fowler, A.G., and P. Jones 1991, "Simulation of Water Quality in Water Distribution Systems," Proceedings Water Quality Modeling in Distribution Systems, Feb, 1991.
- Fluent, Inc., 2005a, FLUENT 6.2 User's Guide, Fluent, Inc., Lebanon, NH, January 2005.
- Fluent, Inc., 2005b, "Modeling Turbulence," Chapter 11 of FLUENT 6.2 User's Guide, Fluent, Inc., Lebanon, NH, January 11, 2005.
- Ho, C.K., L. O'Rear, J.L. Wright, and S.A. McKenna, 2006, "Contaminant Mixing at Pipe Joints: Comparison between Experiments and Computational Fluid Dynamics Models." 8<sup>th</sup> Annual Water Distribution System Analysis Symposium, Cincinnati, Ohio, USA. Aug. 27-30.
- Kim, S-E., 2004, "Large Eddy Simulation Using Unstructured Meshes and Dynamic Subgrid-Scale Turbulence Models," AIAA Paper 2004-2548, 34<sup>th</sup> AIAA Fluid Dynamics Conf and Exhibit, June 28-July 1, Portland, OR.
- Kim, S.-E., and L.S. Mohan, 2005, "Prediction of Unsteady Loading on a Circular Cylinder in High Reynolds Number Flows Using Large Eddy Simulation," OMAE Paper 2005-67044, 24<sup>th</sup> International Conference on Offshore Mechanics and Arctic Engineering, June 12-16, Halkidiki, Greece.
- Kim, S.-E., 2006, "Large Eddy Simulation of Turbulent Flow Past a Circular Cylinder in Subcritical Regime" AIAA Paper 2006-1418, 44th Aerospace Sciences Meeting and Exhibit, January 9-12, 2006, Reno, Nevada.
- Kim, S.-E., and H. Nakamura, 2006, "Large Eddy Simulation of Turbulent Heat Transfer Around a Circular Cylinder in Crossflow," 13<sup>th</sup> International Heat Transfer Conference, Sydney, Australia, August 13-18.
- Lesieur, M. and O. Metais, 1996, "New trends in large-eddy simulations of turbulence," ARFM, 28:45-82.
- Moin P., and K. Mahesh, 1998, "Direct Numerical Simulation: A Tool in Turbulence Research," Annual Reviews in Fluid Mechanics, 30:539-578.
- O'Rear, L., G. Hammond, S.A. McKenna, P. Molina, R. Johnson, T. O'Hern, and B.G. van Bloemen Waanders, 2005, "Physical Modeling of Scaled Water Distribution Systems Networks," SAND2005-676, Sandia National Laboratories, Albuquerque, NM.
- Piomelli, U. and E. Balaras, 2002, "Wall-Layer Models for Large Eddy Simulations," ARFM, 34:349-374.
- Pope, S.B., 2000, Turbulent Flows, Cambridge University Press, Cambridge.
- Romero-Gomez, P., C. Y. Choi, B. G. van Bloemen Waanders, and S. A. McKenna, 2006, "Transport Phenomena at Intersections of Pressurized Pipe Systems," 8<sup>th</sup> Annual Water Distribution System Analysis Symposium, Cincinnati, Ohio, USA. Aug. 27-30.
- Rossman, L., 2000, *EPANET-User's Manual*. United States Environmental Protection Agency (EPA), Cincinnati, OH.
- Sagaut, P., 2004, Large Eddy Simulation for Incompressible Flows – An Introduction, Second Edition, Springer.
- Smagorinski, J., 1963, "General Circulation Experiments with the Primitive Equations. I. The Basic Experiment," *Month. Wea. Rev.*, 91:99-164.
- Tennekes H. and J.L. Lumley, 1972, A First Course in Turbulence, The MIT Press.
- van Bloemen Waanders, B, and G. Hammond, J. Shadid, S. Collis, R. Murray, 2005, "A Comparison of Navier Stokes and Network Models To Predict Chemical Transport in

Municipal Water Distribution Systems,” World Water & Environmental Resources Congress, Anchorage, AL, May 15-19, 2005.

Webb, S.W., and J.T. Cook, 2006, “LES Data-Model Comparisons for Flow Over a Tube Bundle Including Heat Transfer,” 13<sup>th</sup> International Heat Transfer Conference, Sydney, Australia, August 13-18.